Simultaneously harvesting mechanical and chemical energies by a hybrid cell for self-powered biosensors and personal electronics†

Ya Yang,[a] Hulin Zhang,[a] Jun Chen,[a] Sangmin Lee,[a] Te-Chien Hou[a] and Zhong Lin Wang[*ab]

Electrochemical cells (ECs) are devices that convert chemical energy into electricity through spontaneous oxidation–reduction reactions that occur separately at two electrodes through the transport of protons in the electrolyte solution and the flow of electrons in the external circuit. A triboelectric nanogenerator (TENG) is an effective device that converts mechanical energy into electricity using organic/polymer materials by a contact induced electrification process followed by charge separation. In this paper, we demonstrate the first integration of an EC and a TENG for simultaneously harvesting chemical and mechanical energy, and its application for powering a sensor and even personal electronics. An EC was fabricated using a Cu/NaCl solution/Al structure, on which a thin polydimethylsiloxane (PDMS) film with a micropyramid surface structure was used as the protection layer of the EC for anti-corrosion, anti-contamination and anti-mechanical damage. A TENG was fabricated based on a contact-and-separation process between the PDMS protection layer and the Al electrode layer of the EC. The output performance of the TENG can be increased by embedding $BaTiO_3$ nanoparticles into the PDMS film layer to enhance the dielectric property. Moreover, we also demonstrated that the produced hybrid energies can be stored in a Li-ion battery for lighting up 30 green LEDs.

Introduction

Developing renewable and green energy technologies has attracted considerable interest due to the growing energy crisis

[a]School of Materials Science and Engineering, Georgia Institute of Technology, Atlanta, Georgia 30332-0245, USA. E-mail: zlwang@gatech.edu
[b]Beijing Institute of Nanoenergy and Nanosystems, Chinese Academy of Sciences, China

† Electronic supplementary information (ESI) available: Additional figures include the photograph of the fabricated hybrid energy cell, the SEM image of the Si micropyramid template, cross-sectional SEM image of the fabricated PDMS film, XRD patterns of $BaTiO_3$ nanoparticles, the measured output voltage and current density of the composite film, the enlarged output current of the electrochemical cell, the schematic diagram of the self-powered H_2O_2 biosensor, photograph of the biosensor, SEM image of the fabricated Pt electrode, and the enlarged discharging curve of the Li-ion battery. See DOI: 10.1039/c3ee40764k

Broader context

Electrochemical cells (ECs) are devices that convert chemical energy into electricity through spontaneous oxidation–reduction reactions that occur separately at two electrodes through the transport of protons in the electrolyte solution and the flow of electrons in the external circuit. A triboelectric nanogenerator (TENG) is an effective structure that converts mechanical energy into electricity using organic/polymer materials by a contact induced electrification process followed by charge separation. In this work, we demonstrate the first integration of an EC and a TENG for simultaneously harvesting chemical and mechanical energy, and its application for powering a sensor and even personal electronics.

and global warming.[1,2] For the fabrication of any electricity generators, two groups of materials are indispensable. The first group is the action materials that exhibit optoelectronic, piezoelectric, thermal electric and/or pyroelectric properties for converting various forms of energy into electricity.[3–6] The second group is the electrode materials for charge transport. The mechanism of an electrochemical cell (EC) for converting chemical energy into electricity is usually based on spontaneous oxidation–reduction reactions at two different metal electrodes, respectively, in the electrolyte solution to drive electrons to flow in the external circuit.[7,8] Since the supply of water is abundant we do not have to worry about the depletion of the electrolyte. A triboelectric nanogenerator (TENG) has been extensively reported to harvest mechanical energy from irregular mechanical vibrations.[9–11] The mechanism of the TENG is based on the contact–separation between two different triboelectric materials such as polymers or metal materials to induce the electrification and a voltage drop, respectively, which can drive electrons to flow in the external circuit. Usually, each type of energy converter has its own electrodes. An interesting question is whether the electrode materials for two distinctly different devices can be shared. Moreover, to avoid the possible corrosion, contamination and mechanical damage, these devices are usually covered by a protection layer, which may be used as a component to fabricate another energy harvesting unit, such as a TENG.

The purpose of developing hybrid energy cells for self-powered nanotechnology is to use the hybrid energy cells to power some small electronic devices or achieve some electrochemical applications.[12] Although some attempts of the hybrid energy cells have been demonstrated,[13–15] there is no report about the hybrid mechanical and chemical energies for driving the biosensors and personal electronics. Here, we demonstrate the first integration of the EC and the TENG as a hybrid energy cell for harvesting the chemical and mechanical energies. By using the spontaneous oxidation–reduction reactions, an EC was designed to harvest the chemical energy, where the Cu and Al films were used as both the electrode materials and the energy harvesting materials. A polydimethylsiloxane (PDMS) film was covered on the Al electrode of the EC to make a TENG for harvesting mechanical energy, where the PDMS film was used as not only the triboelectric material for the TENG, but also the protection layer of the EC. The output performance of the TENG can be enhanced by embedding of $BaTiO_3$ nanoparticles into the PDMS matrix film. The hybrid energy cell has been used for driving biosensors and lighting up to 30 green LEDs.

Experimental

Fabrication of the hybrid energy cell

A textured Si wafer with micropyramids was created by KOH etching at 353–358 K for 20–30 min. The etching solution was composed of KOH (2 wt%), water, and isopropyl alcohol (5 vol%). The obtained Si micropyramid template was washed by deionized water and dried at room temperature. PDMS (Sylgard 184, Dow Corning) was used as the imprinted polymer, which was prepared by the gel-casting technique. The solution of mixed base monomer and curing agent in a mass ratio of 10 : 1 was dropped on the surface of the Si micropyramid template. The air remaining in the PDMS was removed by a vacuum process. The PDMS film layer was peeled off from the Si micropyramid template after it was kept in the oven at 358 K for 1 h to get cured. The $BaTiO_3$–PDMS composite film was fabricated by embedding of $BaTiO_3$ nanoparticles into the PDMS matrix film. The fabricated hybrid energy cell consists of a TENG and an EC. The TENG device is based on the contact–separation between the fabricated PDMS film and the Al film electrode, where the contact and separation were controlled by using a homemade force loading system with the working frequency of 1 Hz. The EC consists of the Cu film, the NaCl solution (3 wt%), and the Al film.

Measurement of the device

The output voltage of the hybrid energy cell was measured by a low-noise voltage preamplifier (<3 V, Stanford Research SR570; >3 V, Keithley 6514 System Electrometer). The output current of the NGs was measured by a low-noise current preamplifier (Stanford Research SR560). In the H_2O_2 biosensor measurement process, two flexible platinum foils were fabricated by depositing Pt on the flexible PDMS film, serving as the counter electrode and working electrode, respectively. They were employed to detect H_2O_2 molecules in the PBS (phosphate buffer solution,

pH = 7.4) with a concentration of 0.1 M. The hybrid energy cell was used as the power source to drive the biosensor. All experiments were performed at room temperature. The performance of the Li-ion battery was measured by a battery analyzer (MTI Corporation).

Results and discussions

Fig. 1a shows a schematic diagram of the fabricated hybrid energy cell. An Al film was used as a common electrode for both the TENG and the EC. The EC was fixed on a wood structure that was located on the surface of the NaCl solution. The top TENG consists of a Cu film electrode, a PDMS film, and the Al film. The corresponding photograph of the fabricated hybrid energy cell is shown in Fig. S1.† In this study, the PDMS film with a micropyramid surface was fabricated using a Si micropyramid template (Fig. S2†), which was used to enhance the electrification process in the tribo-contacting for the TENG. The detailed fabrication method of the PDMS film is given in the Experimental Section. Fig. 1b shows a scanning electron microscopy (SEM) image of the fabricated PDMS film, revealing that the surface of the film has a micropyramid structure, which was confirmed further by the cross-sectional SEM image of the PDMS film, as shown in Fig. S3† and 1c. The thickness of the PDMS film is about 350 μm. The bottom EC consists of the Al film, the NaCl–water solution, and the Cu film (Fig. 1a).

The mechanical energy applied to the device was harvested using the TENG. Fig. 1d shows the output performance of the fabricated TENG, where the open circuit voltage and the short circuit current density are 11 V and 21.2 nA cm^{-2}, respectively. In this study, the mechanism of the TENG is based on the electrostatic charges generated in the contact–separation process between the PDMS film and the Al film due to the triboelectric effect.[16] When the PDMS is in contact with the Al film, the surface charges will be transferred from Al to PDMS due to the different triboelectric coefficients.[17,18] The separation of the Al from PDMS produces an open circuit voltage, which drives the electrons to flow in the external circuit in order to create an opposite voltage for balancing the one from the triboelectric charges, resulting in the observed output signals. The output open circuit voltage V_{oc} of TENG can be expressed by

$$V_{oc} = \frac{(-\sigma_0 - \sigma_1) \cdot d_S}{\varepsilon_0} - \frac{\sigma_1 \cdot d_{PDMS}}{\varepsilon_0 \varepsilon_r} \quad (1)$$

where σ_0 is the triboelectric charge density, σ_1 is the transferred charge density on the Cu electrode of the PDMS film, d_S is the interlayer distance, d_{PDMS} is the thickness of the PDMS film, ε_0 is the vacuum permittivity, and ε_r is the relative permittivity of the PDMS layer.[16] It is noticed that the σ_0 and σ_1 have the negative and positive values, respectively.

According to eqn (1), the output voltage V_{oc} can increase with increasing relative permittivity ε_r of PDMS. In order to increase the relative permittivity ε_r of the PDMS film, we fabricated a composite made of $BaTiO_3$ nanoparticles in a PDMS matrix. Fig. 2a shows an SEM image of the $BaTiO_3$ nanoparticles, indicating that the diameters of these particles are smaller than 1 μm. X-ray diffraction (XRD) investigations of the obtained
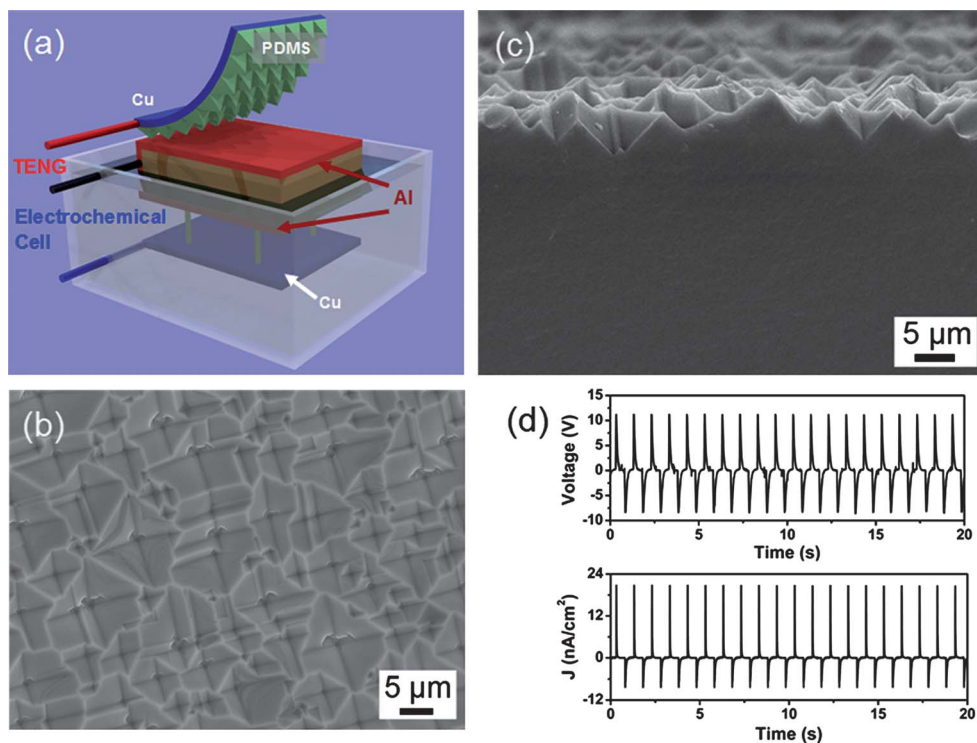
Fig. 1 (a) Schematic diagram of the fabricated hybrid energy cell. (b) SEM image of the obtained PDMS film with the micropyramid surface. (c) Cross-sectional SEM image of the PDMS film. (d) The output open circuit voltage and the output short circuit current density of the fabricated TENG.
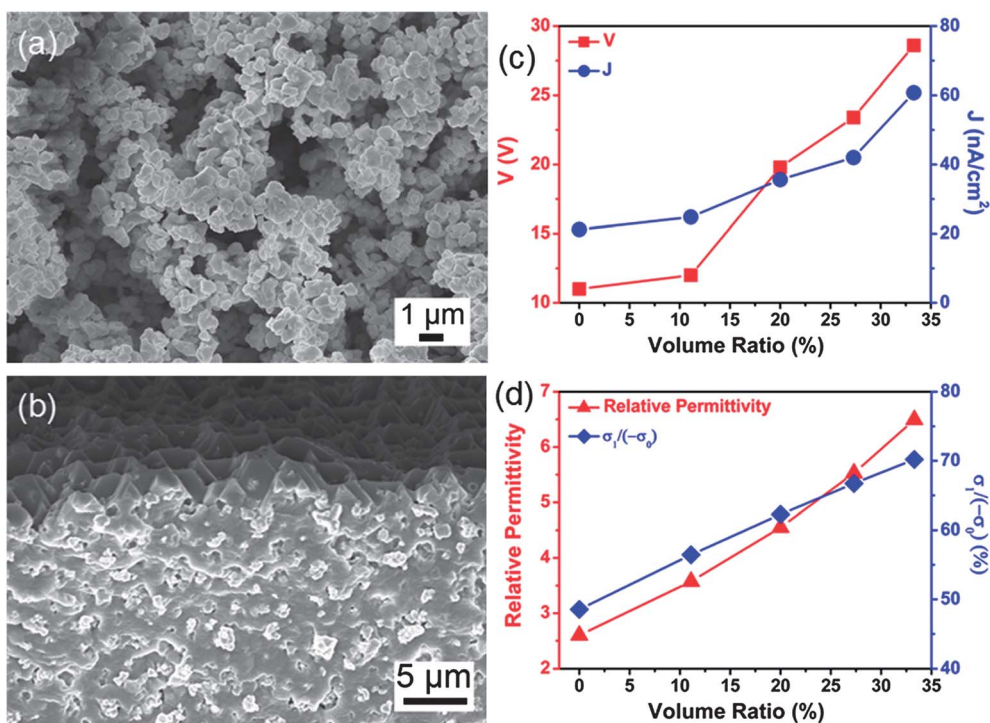
Fig. 2 (a) SEM image of the BaTiO$_3$ nanoparticles. (b) Cross-sectional SEM image of the BaTiO$_3$–PDMS composite film with the volume ratio of BaTiO$_3$ nanoparticles up to 33.3%. (c) Measured output voltage and current of the TENG for the PDMS film composited with different volume ratios of BaTiO$_3$ nanoparticles. (d) Dependence of the relative permittivity and the ratio $\frac{\sigma_1}{-\sigma_0}$ on the volume ratio of the embedded BaTiO$_3$ nanoparticles.

nanoparticles indicate that all of the peaks are perfectly indexed as the cubic phase of $BaTiO_3$, as shown in Fig. S4.† The cross-sectional SEM image of the $BaTiO_3$–PDMS composite film in Fig. 2b shows that the distribution of $BaTiO_3$ nanoparticles in the PDMS matrix is uniform. Fig. S5† shows the output performance of the fabricated composite film-based TENG with a volume ratio (33.3%) of $BaTiO_3$ nanoparticles, where the output voltage and the output current density are 28.6 V and 60.8 nA cm^{-2}, respectively. As compared with the output of a TENG made of a PDMS film without $BaTiO_3$ nanoparticles in Fig. 1d, the output power of the $BaTiO_3$–PDMS composite film-based TENG was increased by about 7 times.

Fig. 2c shows the measured output voltage and the output current density of the $BaTiO_3$–PDMS composite film-based TENG with different volume ratios of $BaTiO_3$ nanoparticles. It can be clearly seen that both the output voltage and the output current density of TENG can increase with increasing the volume ratio of $BaTiO_3$ nanoparticles. According to the Maxwell model, the relative permittivity $\varepsilon_{r(composite)}$ of the $BaTiO_3$–PDMS composite material can be given by

$$\varepsilon_{r(composite)} = \varepsilon_{r(PDMS)} \left[1 + \frac{3\phi_f}{\dfrac{\varepsilon_{r(BTO)}/\varepsilon_{r(PDMS)} + 2}{\varepsilon_{r(BTO)}/\varepsilon_{r(PDMS)} - 2} - \phi_f} \right] \quad (2)$$

where $\varepsilon_{r(PDMS)}$ is the relative permittivity of the PDMS, $\varepsilon_{r(BTO)}$ is the relative permittivity of the $BaTiO_3$ nanoparticles, and ϕ_f is the volume ratio of $BaTiO_3$ nanoparticles in the composite material.[19] According to eqn (2), we can obtain the relative permittivity $\varepsilon_{r(composite)}$ of the $BaTiO_3$–PDMS composite film, as

shown in Fig. 2d. It can be seen that the relative permittivity $\varepsilon_{r(composite)}$ can increase from 2.6 to 6.5 on increasing the volume ratio of $BaTiO_3$ nanoparticles from 0% to 33.3%. According to eqn (1), the first term is independent of ε_r, but the second term is associated with the $\varepsilon_{r(composite)}$. The increase of the relative permittivity $\varepsilon_{r(composite)}$ can effectively increase the output voltage of the TENG, which is consistent with the measured voltages in Fig. 2c. According to eqn (1) and (2), the ratio $\dfrac{\sigma_1}{-\sigma_0}$ between the total transferred charge density σ_1 and the triboelectric charge density σ_0 at the equilibrium state can be given by

$$\frac{\sigma_1}{-\sigma_0} = \frac{d_s}{d_s + d_{PDMS}/\varepsilon_{r(composite)}} \quad (3)$$

According to eqn (3), the obtained ratio $\dfrac{\sigma_1}{-\sigma_0}$ can increase with increasing relative permittivity $\varepsilon_{r(composite)}$ of the $BaTiO_3$–PDMS composite material, as shown in Fig. 2d. Under the same triboelectric charge density, the increase of the total transferred charge density σ_1 can result in the increase of the output current density, which is consistent with the measured output current density in Fig. 2c. Here, the $BaTiO_3$ nanoparticles were used due to their high permittivity. In fact, the other nanomaterials with high permittivity can also be used in the TENG.

The chemical energy in the electrolyte was harvested using the EC. Fig. 3a and b show the output voltage and the output current of the fabricated Cu/NaCl solution/Al-based EC under the forward and reversed connections to the measurement system, respectively. The output voltage is about 0.55 V and there is an obvious output current peak of about 3 mA, which is
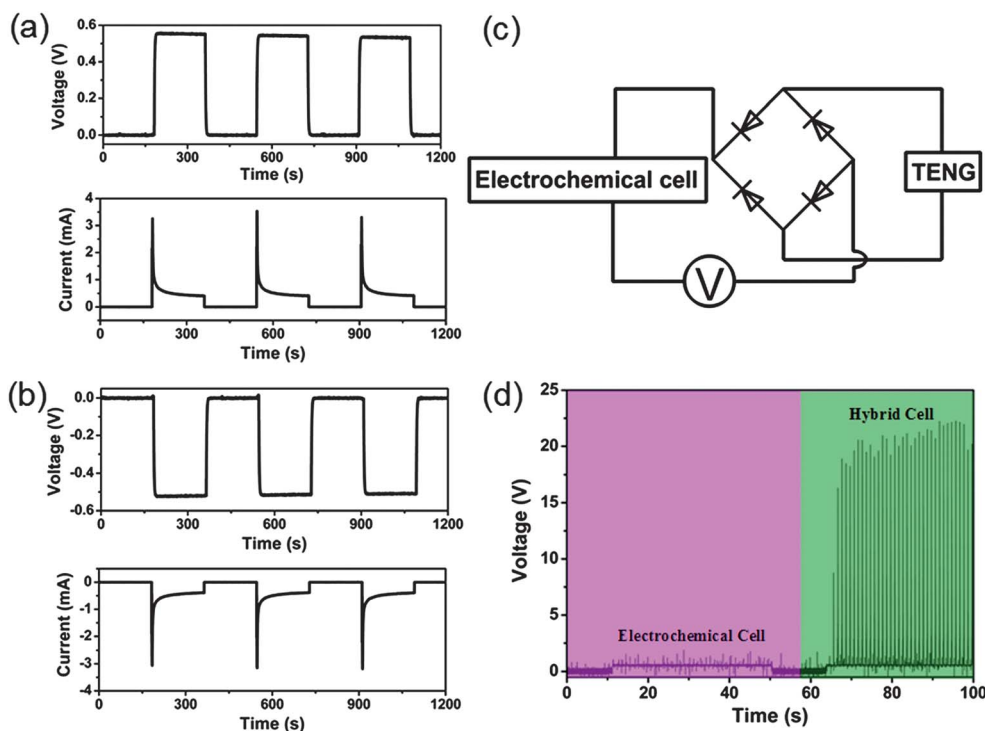

Fig. 3 The output open-circuit voltage and short-circuit current of the fabricated EC under the forward (a) and reversed (b) connections to the measurement system. (c) Schematic diagram of the connection between the TENG and the EC. (d) Measured output open-circuit voltage of the hybrid TENG (after rectification) and EC.
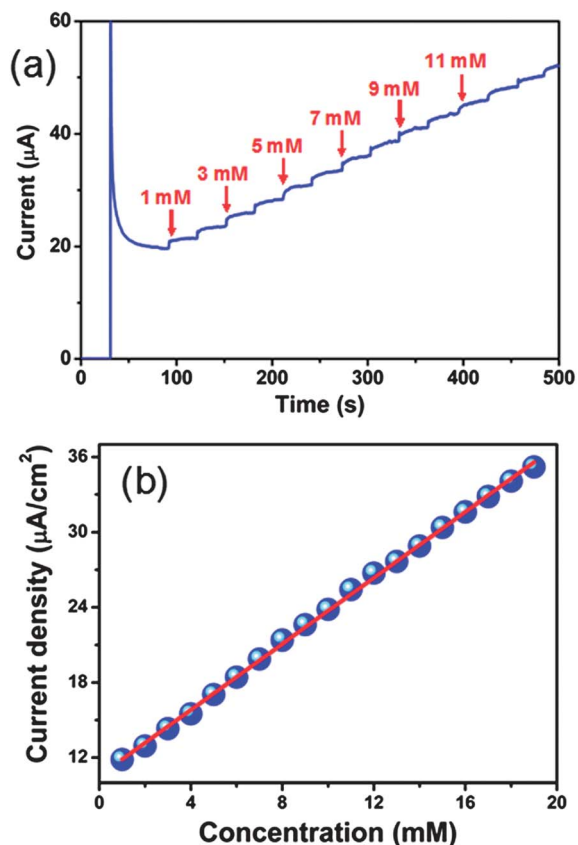
Fig. 4 (a) Current response of the fabricated biosensor to the H_2O_2 molecules with different concentrations. (b) The plot of the response current density *versus* the H_2O_2 concentration in PBS (pH 7.4).

associated with the charge–discharge process of the capacitance induced by the ON/OFF switch in the circuit, where the stable output current is about 0.4 mA (the output current density of 13.3 μA cm^{-2}), as shown in Fig. S6.† The mechanism of the fabricated EC is proposed as follows:

$$2Al - 6e^- \rightarrow 2Al^{3+}(\text{cathode}) \quad (4)$$

$$6H_2O + 6e^- \rightarrow 6OH^- + 3H_2(\text{anode}) \quad (5)$$
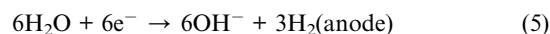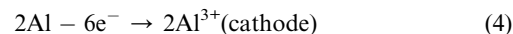
where the oxidation and reduction reactions occur at the cathode and anode, respectively. The spontaneous oxidation–reduction reactions in the NaCl solution can drive electrons to flow in the external circuit, resulting in the observed output voltage and current in Fig. 3a and b.

Fig. 3c shows a schematic diagram of the hybrid energy cell including the TENG and the EC, where the TENG was connected with a bridge rectification circuit for converting alternating current to direct current. Fig. 3d shows the output voltage of the hybrid energy cell. It can be seen that all of the output voltage signals for the hybrid cell are positive and are larger than that of the individual energy harvesters.

To illustrate the potential applications of the hybrid energy cell, we demonstrated that the energies produced by the fabricated hybrid energy cell can be used for directly driving a hydrogen peroxide (H_2O_2) biosensor. Fig. S7† shows the schematic diagram of the self-powered H_2O_2 biosensor, where the TENG and the EC were connected in parallel. The corresponding photograph of the biosensor is shown in Fig. S8.† In this study, we used the Pt electrode as the sensitive electrode material for detecting the H_2O_2. Fig. S9† shows a SEM image of
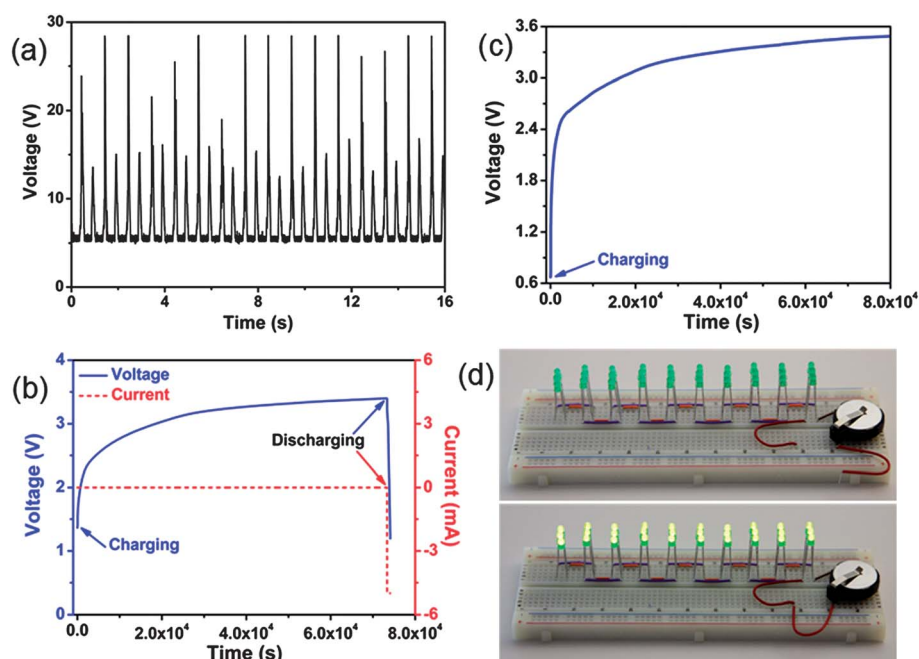
Fig. 5 (a) Measured output voltage of the fabricated hybrid energy cell. (b) The hybrid energy cell charging and the subsequent discharging curves of a Li-ion battery at a constant current. (c) The charging curve of another Li-ion battery. (d) Optical images of 30 green LEDs before and after they were driven by the charged Li-ion battery in (c).

the fabricated Pt electrodes on a PDMS film, revealing that the sizes of the Pt particles are smaller than 1 μm. Fig. 4a shows the continuous current response to the continuous addition of H_2O_2 molecules. It can be clearly seen that the current response of the fabricated sensor increases with increasing concentration of the H_2O_2 molecules. The reaction mechanism of H_2O_2 molecules is proposed as follows:[20]

$$H_2O_2 \xrightarrow{\text{Pt}} 2H^+ + O_2 + 2e^- \text{(anode)} \qquad (6)$$

$$H_2O_2 + 2e^- \rightarrow 2OH^- \text{(cathode)} \qquad (7)$$
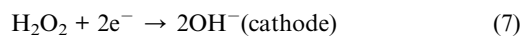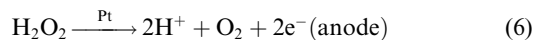
According to eqn (6) and (7), the oxidation and reduction of H_2O_2 molecules occur at the anode and cathode, respectively. This contributes to the increase of the current shown in Fig. 4a, thus the concentration of H_2O_2 molecules can be detected. Fig. 4b shows the linear response range of the biosensor to the H_2O_2 molecules, where the detection concentration can be up to about 20 mM.

To demonstrate more potential applications of the hybrid energy cell, it is necessary to store the energy produced by the hybrid energy cell by using some energy storage units such as Li-ion batteries. Fig. 5a shows the output voltage of the hybrid energy cell up to 28 V, where 15 ECs were integrated in series to increase the output voltage of about 6 V. Fig. 5b shows the charging of the hybrid energy cell and the subsequent discharging curves of a Li-ion battery at a constant current. It can be seen that the Li-ion battery can be charged from 1.4 to 3.4 V with the used time of about 20 h. The enlarged discharging curve in Fig. S10† shows that the discharging of the battery can last for about 700 s before it gets back to the original value of 1.4 V, where the constant discharging current is about 5 mA. The stored electric capacity is about 0.972 mAh. Fig. 5c shows the charging curve of another Li-ion battery, where it can be charged from 0.7 to 3.5 V. The charged Li-ion battery can be used to drive 30 green LEDs, as shown in Fig. 5d. The movie file I (see the ESI†) also shows that the 30 green LEDs can work under the connection with the charged Li-ion battery.

Conclusions

We have demonstrated a hybrid energy cell, which can simultaneously harvest mechanical and chemical energies for driving biosensors and personal electronics. A TENG was fabricated based on the contact–separation between a PDMS layer and the Al electrode layer to harvest mechanical energy. The output performance of the TENG can be increased by adding $BaTiO_3$ nanoparticles in the PDMS matrix to enhance the dielectric property of the PDMS layer. By using the spontaneous oxidation–reduction reactions at two different metal electrodes in the electrolyte solution, we fabricated a Cu/NaCl solution/Al-based EC to harvest chemical energy. Both the TENG and the EC share the Al electrode and the PDMS layer. A H_2O_2 biosensor and the

30 green LEDs can be driven by the hybrid energy cell. The fabricated hybrid energy cells have potential applications in some self-powered electrochemical reactions and driving some personal electronics.

Acknowledgements

Notes and references

1 L. B. Brentner, J. Peccia and J. B. Zimmerman, *Environ. Sci. Technol.*, 2010, **44**, 2243–2254.

2 Y. Yao, K. Huo, L. Hu, N. Liu, J. J. Cha, M. T. McDowell, P. K. Chu and Y. Cui, *ACS Nano*, 2011, **5**, 8346–8351.

3 S. Jeong, E. C. Garnett, S. Wang, Z. Yu, S. Fan, M. L. Brongersma, M. D. McGehee and Y. Cui, *Nano Lett.*, 2012, **12**, 2971–2976.

4 X. Chen, S. Xu, N. Yao and Y. Shi, *Nano Lett.*, 2010, **10**, 2133–2137.

5 C. Chang, V. H. Tran, J. Wang, Y.-K. Fuh and L. Lin, *Nano Lett.*, 2010, **10**, 726–731.

6 Y. Yang, S. Wang, Y. Zhang and Z. L. Wang, *Nano Lett.*, 2012, **12**, 6408–6413.

7 M. Bresadola, *Brain Res. Bull.*, 1998, **46**, 367–380.

8 J. F. Keithley, *Daniell Cell*, ISBN 0-7803-1193-0, John Wiley and Sons, 1999, pp. 49–51.

9 Z. Guang, C. Pan, W. Guo, C.-Y. Chen, Y. Zhou, R. Yu and Z. L. Wang, *Nano Lett.*, 2012, **12**, 4960–4965.

10 F.-R. Fan, Z.-Q. Tian and Z. L. Wang, *Nano Energy*, 2012, **1**, 328–334.

11 F.-R. Fan, L. Long, G. Zhu, W. Wu, R. Zhang and Z. L. Wang, *Nano Lett.*, 2012, **12**, 3109–3114.

12 Z. L. Wang, *Nano Today*, 2010, **5**, 512–514.

13 B. J. Hansen, Y. Liu, R. Yang and Z. L. Wang, *ACS Nano*, 2010, **4**, 3647–3652.

14 C. Xu and Z. L. Wang, *Adv. Mater.*, 2011, **23**, 873–877.

15 Y. Yang, H. Zhang, G. Zhu, S. Lee, Z.-H. Lin and Z. L. Wang, *ACS Nano*, 2013, **7**, 785–790.

16 J. Zhong, Q. Zhong, F. Fan, Y. Zhang, S. Wang, B. Hu, Z. L. Wang and J. Zhou, *Nano Energy*, DOI: 10.1016/j.nanoen.2012.11.015.

17 J. A. Cross, *Electrostatics: Principles, Problems and Applications*, Adam Hilger, Bristol, 1987, ch. 2.

18 E. Nemeth, V. Albrecht, G. Schubert and F. Simon, *J. Electrost.*, 2003, **58**, 3–16.

19 K. Manoli, P. Oikonomou, E. Valamontes, I. Raptis and M. Sanopoulou, *J. Appl. Polym. Sci.*, 2012, **125**, 2577–2584.

20 X. He, C. Hu, H. Liu, G. Du, Y. Xi and Y. Jiang, *Sens. Actuators, B*, 2010, **144**, 289–294.